Recursive modal parameter estimation using output-only subspace identification for structural health monitoring

Kashif Saeed, Nazih Mechbal, Gérard Coffignal, Michel Vergé

Recursive Modal Parameter Estimation using Output-only Subspace Identification for Structural Health Monitoring

Kashif Saeed*, Nazih Mechbal, Gérard Coffignal and Michel Vergé
*Arts et Metiers ParisTech, UMR-CNRS 8106, LMSP
151 bd de l'Hopital 75013 PARIS, France
Email: kashif.saeed-5@etudiants.ensam.fr

***Abstract*— Precise identification of structural properties is a vital step towards detection and localization of damage in structures. In this paper the problems of improving accuracy of modal parameter estimates and automatic elimination of spurious modes in covariance driven output-only subspace identification method are addressed. An iterative procedure is proposed, which in the first step, actively modifies the excitation signal, resulting in improvements in identification results. In the second step, for spurious mode elimination, an alternative stabilization histogram is introduced to automatically combine and extract identified modal parameters. It is shown that use of measured output signals, of different sampling rates, along with combination of identified results on a single stabilization histogram, can enhance the effectiveness of spurious modes rejection. One numerical and two experimental examples, on the modal parameter estimation of a composite beam and an aluminum plate (CACTUS) are presented to demonstrate the efficacy of the iterative procedure. The proposed algorithm allows automatic and accurate generation of modal parameter residuals for structural health monitoring applications.**

I. Introduction

Detecting and localizing damage in smart structures is a topic of growing interest in Structural Health Monitoring (SHM) [1], [2], [3]. These structures have built in piezoelectric sensors and actuators, which can be used to identify the changes caused by damage in structural parameters, such as modal properties. The sensitivity and use of modal properties for damage detection have been extensively studied [4], [5] and many modal parameter identification methods have been proposed. One of the modal parameter identification methods, which has gained popularity in recent years, is Subspace Based Identification (SubID) [6].

SubID methods estimate the state-space sequence using input/output signals. The original SubID method is non-iterative and is restricted only to offline implementation because of computational complexity of robust matrix operations such as singular value decomposition (SVD). Moreover, like many other identification methods, SubID depends heavily on excitation force. Weak ambient excitations along with ambient noise have strong influence on the accuracy of estimates. In order to benefit from ambient excitation, long samples are used with models of redundant order. However, using model of redundant order generates spurious modes, which mix intensively with physical modes, making them difficult to identify. It has been observed that as the model order is increased, the physical modes tend to stabilize as compared to the spurious ones. This is the core idea behind stabilization diagrams [7], [8], which exhibit the variation of modal parameters relative to increments in modal order, making them an effective tool for spurious mode identification. However, they require extensive user interaction as some numerical spurious modes behave as physical ones, when the model order is changed making them very difficult to identify on stabilization diagrams.

In order to reduce computation complexity, recursive SubID algorithms have been proposed. Mercère et al [9] and Delgado et al [10] have developed methods that identify system matrices without extracting state sequence information. Whereas, Pongpairoj and Pourboghrat [11] estimated state sequences from approximated subspace intersection of sequential updated vector. Methods [12], [13] have been proposed to reinforce stabilization diagrams but they do not eliminate spurious modes automatically. Therefore, the problems of improving the accuracy of modal parameter estimates and the automatic elimination of spurious modes using covariance driven output-only SubID methods are addressed in this paper.

We propose a two step iterative procedure for improving the accuracy of modal parameter estimation on active structures, while using covariance based output-only SubID. In the first step, excitation force is iteratively modified to have a better estimate of the modal parameters. In the second step, an attempt is made to eliminate the spurious modes by using an original stabilization histogram and by resampling of measured output data. In order to reduce the complexity of modal testing and to increase the flexibility of implementation, output-only SubID method was applied.

The paper is organized as follows. A brief introduction to output-only covariance driven SubID algorithm is given in section 2. The proposed algorithm is introduced in section 3. Results from two case studies are demonstrated in section 4 and 5. Section 6 concludes the paper with future prospects.

II. Modal Analysis by Subspace Identification

A. State Space Model

It is generally convenient to convert the second order differential equations of a flexible structure in state-space form. If $1/\tau$ is the sampling rate then the discrete state-space model is given by

$$\underline{x}_{k+1} = \underline{\underline{A}}_d \underline{x}_k + \underline{\underline{B}}_d \underline{u}_k + \underline{w}_k \tag{1}$$

$$\underline{y}_k = \underline{\underline{C}}\, \underline{x}_k + \underline{v}_k \tag{2}$$

where, $\underline{x}_k \in \mathbb{R}^{n_s}$, $\underline{u}_k \in \mathbb{R}^{n_u}$ and $\underline{y}_k \in \mathbb{R}^{n_y}$ are respectively the state-space, input and output vectors at time instant k. n_d is the system order, n_s is state-space order, n_y is the number of outputs and n_u is the number of inputs. $\underline{\underline{A}}_d$, $\underline{\underline{B}}_d$ and $\underline{\underline{C}}$ are the discrete system, input and the output matrices respectively. $\underline{w}_k$ and $\underline{v}_k$ are respectively the process and the measurement noise vectors.

Considering that the system behaves like a stationary linear dynamics system and that input forces can be modeled as a non-stationary white noise, the model can be modified as

$$\underline{x}_{k+1} = \underline{\underline{A}}_d \underline{x}_k + \underline{w}_k \tag{3}$$

$$\underline{y}_k = \underline{\underline{C}}\, \underline{x}_k + \underline{v}_k \tag{4}$$

Here, the process and the measurement noise are assumed to be zero-mean Gaussian white noise processes such as

$$E\left[\begin{bmatrix} \underline{w}_k \\ \underline{v}_k \end{bmatrix} \begin{bmatrix} \underline{w}_k & \underline{v}_k \end{bmatrix}\right] = \begin{bmatrix} \underline{\underline{Q}} & \underline{\underline{S}} \\ \underline{\underline{S}}^T & \underline{\underline{R}} \end{bmatrix} \delta(t) \tag{5}$$

where, E is the expectation operator and $\delta(t)$ is the Kronecker delta. $\underline{\underline{Q}}$ and $\underline{\underline{R}}$ are process and measurement noise covariance matrices. $\underline{\underline{S}}$ is the cross-covariance between process and measurement noise.

B. Output-only Covariance Driven Subspace Identification

Covariance driven SubID is based on the following steps [14]. Let $\underline{\underline{\Lambda}}_i$ be output covariance matrix given by

$$\underline{\underline{\Lambda}}_i = E\left[\underline{y}_{k+i}\underline{y}_k^T\right] \tag{6}$$

A Hankel matrix is constructed using $p+1$ block rows and q block columns of the output covariance matrix.

$$\underline{\underline{H}}_{p+1,q} = \begin{bmatrix} \underline{\underline{\Lambda}}_1 & \underline{\underline{\Lambda}}_2 & \cdots & \underline{\underline{\Lambda}}_q \\ \underline{\underline{\Lambda}}_2 & \underline{\underline{\Lambda}}_3 & \cdots & \underline{\underline{\Lambda}}_{q+1} \\ \vdots & \vdots & \ddots & \vdots \\ \underline{\underline{\Lambda}}_{p+1} & \underline{\underline{\Lambda}}_{p+2} & \cdots & \underline{\underline{\Lambda}}_{p+q+1} \end{bmatrix} \tag{7}$$

Considering that the system is stationary and that the process and measurement noises are white, Gaussian with zero mean, we can rewrite (6) as

$$\underline{\underline{\Lambda}}_i = \underline{\underline{C}}\,\underline{\underline{\Sigma}}\,\underline{\underline{C}}^T + \underline{\underline{R}} \qquad i = 0 \tag{8}$$

$$\underline{\underline{\Lambda}}_i = \underline{\underline{C}}\,\underline{\underline{A}}_d^{i-1}\underline{\underline{G}} \qquad i > 0 \tag{9}$$

where, $\underline{\underline{G}}$ is the cross-covariance between state and observed output. This leads to the factorization of Hankel matrix as

$$\underline{\underline{H}}_{p+1,q} = \underline{\underline{O}}_{p+1}\underline{\underline{\mathbb{C}}}_q \tag{10}$$

where

$$\underline{\underline{O}}_{p+1} = \begin{bmatrix} \underline{\underline{C}} & \underline{\underline{C}}\,\underline{\underline{A}}_d & \cdots & \underline{\underline{C}}\,\underline{\underline{A}}_d^p \end{bmatrix}^T \tag{11}$$

and

$$\underline{\underline{\mathbb{C}}}_q = \begin{bmatrix} \underline{\underline{G}} & \underline{\underline{A}}_d\underline{\underline{G}} & \cdots & \underline{\underline{A}}_d^{q-1}\underline{\underline{G}} \end{bmatrix} \tag{12}$$

are $p+1$ order Observability and q order Controllability matrices of rank n_d respectively.

In order to calculate the system state matrix $\underline{\underline{A}}_d$ the first block row of the observability matrix $\underline{\underline{O}}_{p+1}$ is deleted to get a truncated observability matrix $\underline{\underline{O}}^{\uparrow}_{p+1}$ given by

$$\underline{\underline{O}}^{\uparrow}_{p+1} = \begin{bmatrix} \underline{\underline{C}}\,\underline{\underline{A}}_d & \underline{\underline{C}}\,\underline{\underline{A}}_d^2 \cdots & \underline{\underline{C}}\,\underline{\underline{A}}_d^p \end{bmatrix}^T \tag{13}$$

Thus, the system state matrix $\underline{\underline{A}}_d$ can be calculated by

$$\underline{\underline{A}}_d = \underline{\underline{O}}^{\oplus}_p \underline{\underline{O}}^{\uparrow}_{p+1} \tag{14}$$

where, $\underline{\underline{O}}^{\oplus}_p$ represents the pseudo-inverse of p order observability matrix. The output state matrix $\underline{\underline{C}}$ can be obtained from the first block row of $\underline{\underline{O}}_p$. Thus, the state-space model given in (3) and (4) can be identified.

Modal parameters are estimated by using the output matrix $\underline{\underline{C}}$ and system matrix $\underline{\underline{A}}_d$. Eigenvalues of $\underline{\underline{A}}_d$ yield the natural frequencies f_i and damping ratios ζ_i of the system. Mode-shapes $\underline{\phi}_i$ are obtained in the dimension of the measured degrees of freedom from corresponding eigen-vectors.

C. Balanced Realization

For the time being, we use Balanced Realization [15] for the implementation of SubID, which uses SVD to obtain observability and controllability matrices. In practice, only finite number of samples are available. As a result, the output covariance matrices are calculated by

$$\hat{\underline{\underline{\Lambda}}}_i = \frac{1}{n_\tau - i}\sum_{k=1}^{n_\tau - i} \underline{y}_{k+i}\underline{y}_k^T \tag{15}$$

where, n_τ is the number of samples. Experimental Hankel matrix $\hat{\underline{\underline{H}}}_{p+1,q}$ is populated using the estimated output covariance matrices $\hat{\underline{\underline{\Lambda}}}_i$. The SVD of $\hat{\underline{\underline{H}}}_{p+1,q}$ and its truncation at a desired model order, yields the estimated observability $\hat{\underline{\underline{O}}}_{p+1}$ and controllability $\hat{\underline{\underline{\mathbb{C}}}}_{p+1}$ matrices

$$\hat{\underline{\underline{H}}}_{p+1,q} = \begin{bmatrix} \underline{\underline{U}}_1 & \underline{\underline{U}}_2 \end{bmatrix} \begin{bmatrix} \underline{\underline{S}}_1 & \underline{\underline{0}} \\ \underline{\underline{0}} & \underline{\underline{S}}_2 \end{bmatrix} \begin{bmatrix} \underline{\underline{V}}_1 & \underline{\underline{V}}_2 \end{bmatrix}^T \tag{16}$$

$$\hat{\underline{\underline{O}}}_{p+1} = \underline{\underline{U}}_1\underline{\underline{S}}_1^{1/2} \tag{17}$$

$$\hat{\underline{\underline{\mathbb{C}}}}_{p+1} = \underline{\underline{S}}_1^{1/2}\underline{\underline{V}}_1 \tag{18}$$

III. Recursive Method

For a damage detection algorithm, using changes in modal parameters as an indication of damage, underling modal parameter identification method must be precise and accurate. To achieve this goal, we propose an alternative recursive approach using a stabilization histogram.

A. Stabilization Histogram

Order stabilization diagram exhibits variation of modal parameters estimates with increments in model order. Though increasing model order reveals stability of physical modes but it also increases the interference of spurious modes. There are two types of spurious modes, the ones generated by noise/weak ambient excitation and others resulting from numerical inaccuracies. By far, stabilization diagram is the

most commonly used method for physical mode identification [7] but it requires extensive user interaction as some numerical spurious modes behave like physical ones. In order to automate modal parameter extraction from SubID method, an alternative approach using a histogram is proposed.

To construct a stabilization histogram, we propose first, to categorize the modes in n_c categories. The modes are categorized according to the stability of natural frequencies, damping ratios and modes shapes, with respect to increments in model order. For example, here, we define three categories: stable modes, semi-stable modes and new modes. A mode calculated for a given order is said to be stable if frequency varies less than 1% from the previous order and damping ratio varies less than 5%. Semi-stable modes have stable frequencies but no stable damping coefficients. New modes have neither stable frequency nor stable damping coefficients. Adding a mode shape stability criteria will increase the number of catagories and might improve results.

Weights are associated with each category. The weight of a more stable category is selected to be comparatively higher than all other less stable categories. Considering the previous stated example, the weight of a stable mode is greater than that of a semi-stable mode and the weight of semi-stable mode is greater than the weight of a new mode.

The working frequency band is divided into discrete intervals. With each interval a counter is associated. For an estimated mode that falls in a given frequency interval, the counter is incremented by the weight of the associated category. As a result stable modes will have higher counts as compared to less stable modes. Plotting counts with respect to frequency, results in a histogram that shows higher peaks for more stable modes.

B. Excitation Signal

Results generated by output-only covariance driven SubID method depend heavily on the excitation force, which is considered here to be unknown. In order to improve the results and yet still retain the simplicity of this algorithm, it is in our interest to excite a structure with a well defined input signal but disregard it during the identification process. We propose an iterative procedure, which actively changes this input signal based on the results of previous identification attempts. The procedure is given as follows:

1) Data acquisition from ambient excitation
2) SubID and construction of stabilization histogram
3) Generation of a pseudorandom binary signal having considerable energy around the identified frequencies
4) Data acquisition from forced excitation
5) SubID and construction of stabilization histogram
6) Going to step 3 till the identified frequencies stabilize

We assume that on an active structure the excitation points are well optimized to excite the modes in the working frequency band. We also assume that during the period of algorithm convergence, the structural properties will not change. After the stabilization of input signal, spurious modes should be eliminated so that results can be used for damage detection algorithm.

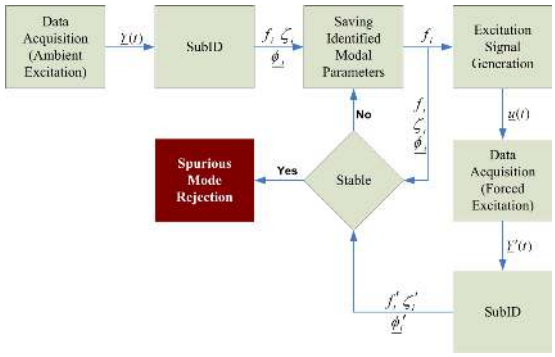

Fig. 1. Online Modal Parameter Estimation using Output-only Subspace Identification.

C. Spurious Mode Rejection

We have observed that as spurious modes generated by noise do not stabilize while increasing the model order, however, the numerical spurious modes do tend to stabilize and can be considered as physical modes of the system. We have also observed that these numerical spurious modes depend on the sampling period. In the second step of spurious mode rejection, we propose to downsample the system output, which was originally measured at a high sampling rate and re-estimate the modal parameters. Injecting these results, from different sampling rates, in a single stabilization histogram reveals spurious modes because physical modes remain stable under both conditions of changing sampling rate and model order. Flow diagram of the proposed algorithms is shown in Fig. 1

IV. Case Studies - Active Composite Beam

The proposed online modal parameter estimation method is applied to an active composite beam structure (Fig. 2). The beam consists of a composite filling covered with two external thin plates. There are three pairs of PZ29 piezoelectric ceramics, bounded symmetrically on both sides of this beam. They are positioned parallel to the mid plate surface and are polarized in a way that permits sensing or generating pure bending motion.

The aim is to accurately and automatically identify the first five natural modes of the structure, using measurements from a single piezoelectric pair and one excitation source. Using output measurements from a single piezoelectric pair restricts us to only consider the stability of natural frequencies and damping coefficients. The categories defined in the example stated in section III will be used for all the results shown in this paper. Weights selected for stable, semi-stable and new modes are 8, 2 and 1 respectively and the frequency interval set to $0.1Hz$.

A. Simulation

A finite element model (FEM) of the beam is constructed using Bernoulli hypothesis, for simulations purposes. The modeled structure is damped satisfying Caughey's criteria [16]. Natural frequencies and the corresponding damping ratios are shown in Table I.

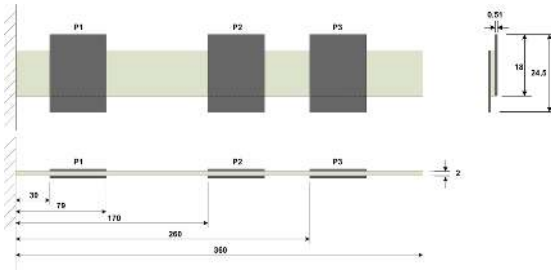

Fig. 2. The Active Composite Beam Structure.

TABLE I
FIRST FIVE MODES OF THE MODELED BEAM

Modes	1^{st}	2^{nd}	3^{rd}	4^{th}	5^{th}
Natural Frequency (Hz)	6.7	44.8	126.2	273.5	490.5
Damping Ratio $\times 10^{-3}$	4	6	7	15	11

The dynamic response of piezoelectric pair 2, to a random signal excitation by piezoelectric pair 1, is simulated using Newmark Integration method. White noise is added on the simulated response with signal to noise ratio of $10dB$.

Stabilization diagram generated after applying SubID to the simulated response data, measure at $2500Hz$, is shown in Fig. 3. The corresponding stabilization histogram is shown in Fig. 4. Both the diagrams show difficulties in identifying the first two modes of the beam. The histogram shows high peaks for the two well identified modes at $273Hz$ and $490Hz$. However, counts for the first two modes are lower as compared to spurious modes. Using the first 15 frequencies, having the highest count, an input signal is generated by the proposed algorithm, in order to better excite the structure in the next iterations.

Five peaks on the stabilization histogram (Fig. 5), obtained after 3^{rd} iteration, correspond well with the first five modes of the beam. As there are no spurious modes, the final estimated values are shown in Table II.

To demonstrate the effectiveness of spurious mode rejection, the proposed algorithm is implemented on an experimental setup.

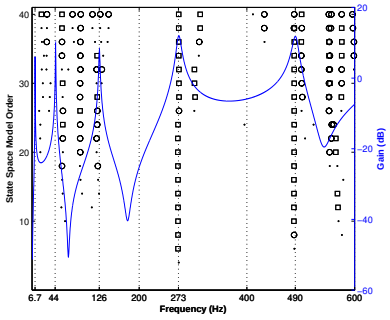

Fig. 3. Stabilization diagram obtained after random excitation of modeled beam after 1^{st} Iteration. Stable, semi-stable and new modes are represented by square, circle and dot respectively. Right y-axis corresponds to Bode diagram obtained from the FEM model.

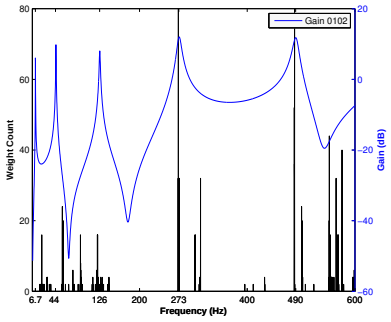

Fig. 4. Stabilization histogram obtained after 1^{st} Iteration from random excitation of modeled beam.

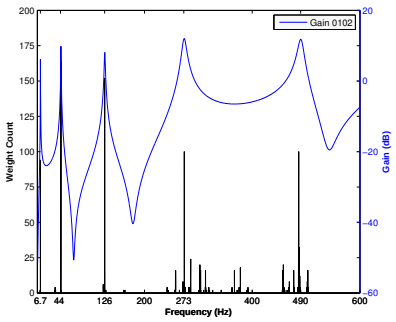

Fig. 5. Stabilization histogram obtained after 3^{rd} iteration.

B. Experimental Setup

The experimental setup is completed by a control loop: charge amplifiers for the conditioning of measurement signals, voltage amplifiers for the actuators and a specialized dSpace© card performing the real time measurements and control. Initially the beam is excited by random signal using the 1^{st} piezoelectric pair as actuator. Vibration data is measured from 2^{nd} piezoelectric sensor at a sampling rate of $10kHz$ for a duration of 2 minutes. This data is downsampled to $1250Hz$ and then used to generate the stabilization diagram and the corresponding histogram, given in Fig. 6 and Fig. 7 respectively. These figures reveal that it is difficult to identify the first and the second modes of the structure. Moreover, there are spurious modes, which stabilize with increasing model order.

The advantage of stabilization histogram is that it not only allows better identification of first mode but also assists in

TABLE II
FIRST FIVE IDENTIFIED MODES OF THE MODELED BEAM

Modes	1^{st}	2^{nd}	3^{rd}	4^{th}	5^{th}
Natural Frequency (Hz)	6.7	44.7	126.6	278.4	486.6
Damping Ratio $\times 10^{-3}$	4.5	3.8	8.0	8.5	10.7

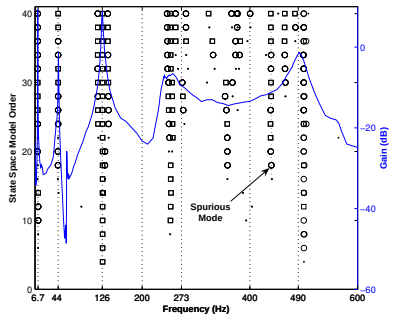

Fig. 6. Stabilization diagram obtained from experimental data measured at a sampling rate of $1250Hz$ with random excitation. Right y-axis corresponds to Bode diagram obtained from manual identification of the beam.

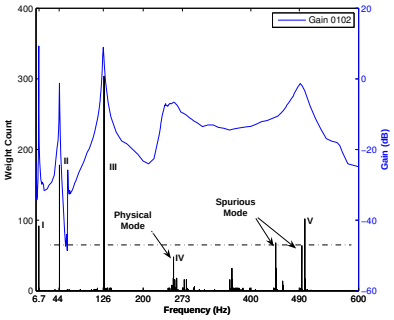

Fig. 7. Stabilization histogram obtained from experimental data measured at a sampling rate of $1250Hz$ with random excitation.

constructing a richer signal for excitation. Exciting the beam with a refined input, generated iteratively, yields the final stabilization diagram shown in Fig. 8

The 4^{th} mode at $257Hz$ is weakly identified and there rests a numerical spurious mode, which stabilizes with increasing model order at $430Hz$. To eliminate the spurious mode, the response is measured at a higher sampling rate of $10kHz$. It shifts the numerical spurious modes to higher frequencies but the task of identifying the low frequency modes becomes more difficult (Fig. 9).

Histograms allow the user to analyze extremely large data

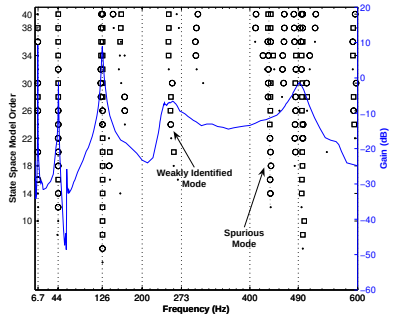

Fig. 8. Stabilization diagram obtained from experimental data measured at a sampling rate of $1250Hz$ with improved excitation

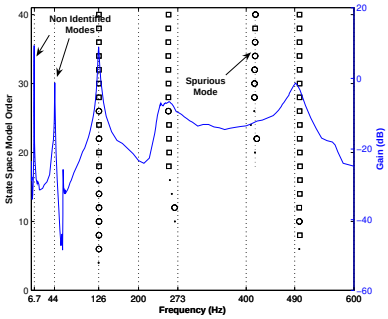

Fig. 9. Stabilization diagram obtained from experimental data measured at a sampling rate of $10kHz$ with improved excitation

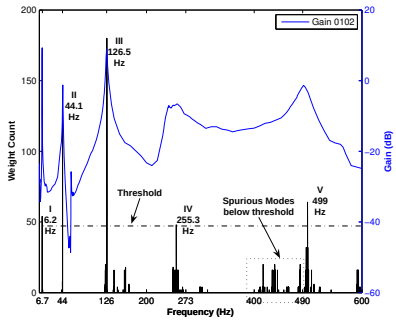

Fig. 10. Combined stabilization histogram

sets by reducing them to a single 1-D graph. Plot obtained by combining the results of both the experiments (Sampling at $1250Hz$ and $10kHz$) in a single stabilization histogram is shown in Fig. 10.

Counts of all the first five vibration modes are well above the selected threshold, allowing them to be automatically selected. Whereas, the effect of the numerical mode is cancelled by changing the sampling period. Final estimated values of the first five modes are shown in Table III.

V. Case Studies - CACTUS

The proposed algorithm is also tested on a thin aluminum plate like structure called CACTUS (Fig. 11). CACTUS is $2mm$ thick and is clamped in vertical position. There are nine pairs of PZ29 piezoelectric ceramics, bounded symmetrically on both sides of the plate.

The aim is to identify the first seven natural modes of the structure up to $55Hz$. Initially, the structure is excited by random signal using the 1^{st} piezoelectric pair as actuator.

TABLE III
First Five Identified Modes of the Composite Beam

Modes	1^{st}	2^{nd}	3^{rd}	4^{th}	5^{th}
Natural Frequency (Hz)	6.2	44.1	126.5	255.5	499.0
Damping Ratio $\times 10^{-3}$	4.2	5.5	6.9	98.4	26.7

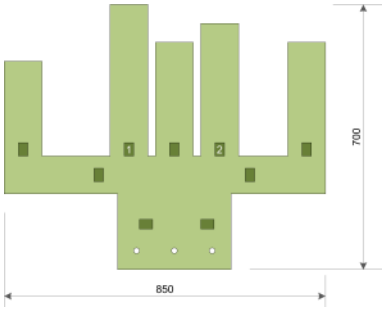

Fig. 11. CACTUS

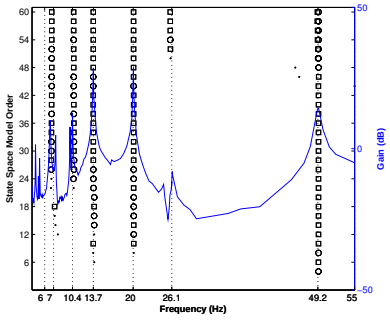

Fig. 12. Stabilization diagram obtained from experimental data obtained from CACTUS, measured at a sampling rate of $1kHz$ with random excitation. Right y-axis corresponds to Bode diagram obtained from manual identification of CACTUS.

Vibration data is measured from 2^{nd} piezoelectric sensor at a sampling rate of $1kHz$ for duration of 1 minute.

Stabilization diagram (Fig. 12) thus obtained, reveals that 2^{nd}, 3^{rd} and 6^{th} modes at $7.7Hz$, $13.7Hz$ and $26.1Hz$ are not identified. The stabilization histogram generated by the proposed algorithm obtained after cancellation of spurious modes on 4^{th} iteration is shown in Fig. 13. The distinct peaks allow the first seven modes to be easily distinguished from the spurious modes.

VI. CONCLUSIONS

Identifiability of modal parameters is enhanced by exciting the structure with a well defined input signal. Spurious modes are eliminated by changing the sampling rate of measured output signal and by combining the results on a single stabilization histogram. The estimated results have show that the proposed algorithms not only allowed automatic selection of excitation signal in small number of iterations but also removed the spurious modes from the generated results. The present approach was applied using a SubID method, which is based on SVD of Hankel matrix, which is computationally complex. For a real-time SHM applications, the underlining identification algorithm should have reduced computational complexity. Next steps in this study are to observe the performance of the proposed algorithms using recursive SubID methods and to analyze their robustness in generating modal parameter residuals for SHM applications.

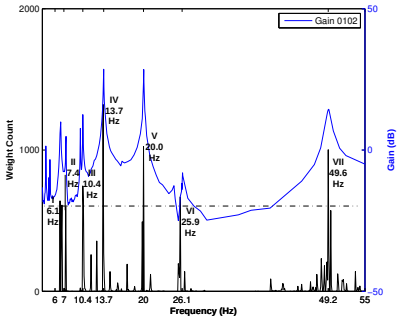

Fig. 13. Stabilization histogram obtained from experimental data obtained from CACTUS.

REFERENCES

[1] W. Lestari, P. Qiao, and S. Hanagud, "Curvature mode shape-based damage assessment of carbon/epoxy composite beams," *Journal of Intelligent Material Systems and Structures*, pp. 1–20, Oct. 2006.

[2] S. Hurlebaus and L. Gaul, "Smart structure dynamics," *Mech Syst Signal Process*, vol. 20, no. 2, pp. 255–281, Feb. 2006.

[3] N. Mechbal, M. Vergé, G. Coffignal, and M. Ganapathi, "Application of a combined active control and fault detection scheme to an active composite flexible structure," *Mechatronics*, vol. 16, no. 3-4, pp. 193–208, 2006.

[4] W. K. and D.-B. J.M., "An overview of intelligent fault detection in system and structures," *Structural Health Monitoring*, vol. 3, no. 1, pp. 85–98, Mar. 2004.

[5] H. Sohn, C. Farrar, H. F.M., D. Shunk, D. Stinemates, and B. Nadler, "A review of structural health monitoring literature: 1996-2001," Los Alamos National Laboratory, Tech. Rep., 2003.

[6] T. Katayama, *Subspace methods for system identification*. Springer, Oct. 2005.

[7] H. Van der Auweraer, W. Leurs, P. Mas, and L. Hermans, "Modal parameter estimation from inconsistent data sets," *Proc Int Modal Anal Conf IMAC*, vol. 1, no. United States, pp. 763–771, 2000.

[8] R. Allemang and D. Brown, "Correlation coefficient for modal vector analysis," in *Proceedings of the International Modal Analysis Conference & Exhibit*, 1982, pp. 110–116.

[9] G. Mercère, S. Lecoeuche, and M. Lovera, "Recursive subspace identification based on instrumental variable unconstrained quadratic optimization," *Int J Adapt Control Signal Process*, vol. 18, no. 9-10, pp. 771–797, 2004.

[10] C. Delgado and P. Dos Santos, "Recursive canonical variate subspace algorithm," in *SICE Annual Conference 2004*, Faculdade de Economia do Porto, Rua Dr. Roberto Frias, 4200-464 Porto, Portugal Fac. de Engenharia, Univ. do Porto, Rua Dr. Roberto Frias, 4200-465 Porto, Portugal, 2004, pp. 2025–2030.

[11] H. Pongpairoj and F. Pourboghrat, "Real-time optimal control of flexible structures using subspace techniques," *IEEE Transactions on Control Systems Technology*, vol. 14, no. 6, pp. 1021–1033, Nov. 2006.

[12] J. Fan, Z. Zhang, and H. Hua, "Data processing in subspace identification and modal parameter identification of an arch bridge," *Mech Syst Signal Process*, vol. 21, no. 4, pp. 1674–1689, May 2007.

[13] B. Cauberghe, P. Guillaume, P. Verboven, S. Vanlanduit, and E. Parloo, "On the influence of the parameter constraint on the stability of the poles and the discrimination capabilities of the stabilisation diagrams," *Mech Syst Signal Process*, vol. 19, no. 5, pp. 989–1014, 2005.

[14] L. Mevel, A. Benveniste, M. Basseville, M. Goursat, B. Peeters, H. Van Der Auweraer, and A. Vecchio, "Input/output versus output-only data processing for structural identification–application to in-flight data analysis," *J Sound Vib*, vol. 295, no. 3-5, pp. 531–552, Aug. 2006.

[15] H. Akaike, "Stochastic theory of minimal realization," *IEEE Trans Autom Control*, vol. AC-19, no. 6, pp. 667–674, 1974.

[16] S. Adhikari, "Damping modelling using generalized proportional damping," *J Sound Vib*, vol. 293, no. 1-2, pp. 156–170, 2006.